

MULTIPLE ALKALI-ENRICHED FELDSPAR GENERATIONS IN FELSITE-CONTAINING LUNAR BRECCIA 12013. R. Christoffersen¹, M. D. Mouser^{1,2}, J. I. Simon², and D. K Ross¹, ¹Jacobs-JETS contract, NASA Johnson Space Center, Mail Code XI3, Houston, TX 77058, USA (roy.christoffersen-1@nasa.gov), ²Dept. of Earth and Planetary Sciences, University of New Mexico, Albuquerque, NM 87131, USA (mmouser@vols.utk.edu), ²Center for Isotope Cosmochemistry and Geochronology, Astromaterials Research & Exploration Science, NASA Johnson Space Center, Houston, TX 77058, USA (justin.i.simon@nasa.gov).

Introduction: As representatives of some of the most petrochemically evolved suites of igneous rocks on the Moon, the granitic felsite clasts in lunar breccias have come under renewed focus as part of new efforts to use feldspars for assessing the inventory of lunar water and other volatiles [1,2,3,4]. Previous petrologic studies of these clasts [5,6], including the post-Apollo work [6], were tilted towards finding those assemblages and relationships most likely to be “pristine”, i.e. direct products of magmatic processes, however simple or complex.

In support of our on-going NanoSIMS measurements of trace water contents in the feldspars in these clasts [1,2], we are using coordinated analytical SEM, electron probe microanalyzer (EPMA) and analytical TEM techniques to re-evaluate the full diversity of processes under which the feldspar-bearing assemblages in these clasts formed [7]. The results reported here for lunar breccia 12013 show multiple stages under which alkali feldspar-plagioclase-silica assemblages were generated, not all of them *sensu stricto* magmatic. This includes a role for shock effects in creating physical/chemical conditions under which alkalis are mobilized to facilitate feldspar crystallization by processes not previously recognized in these rocks.

Methods: Analytical SEM, EPMA and TEM imaging and analyses were performed on polished indium mounts of felsite-containing fragments of lunar breccia 12013 [6]. A JEOL 7600F field-emission SEM with energy-dispersive X-ray (EDS) element mapping capabilities was used to acquire detailed back-scatter electron images and element maps of the entire mounts and key sub-areas of interest. Follow-up quantitative EPMA spot analyses of feldspars were obtained using a JEOL 8530F field-emission EPMA. A JEOL 7600 field-emission scanning transmission electron microscope (FE-STEM) supported by an FEI Quanta dual-beam focused ion beam (FIB) instrument for sample preparation, was used to investigate sub-micron scale microstructural and compositional relations in selected regions.

Results: As originally described by [6], 12013 is notable for its abundant patchy areas of a fine-grained granophyre (microgranophyre) assemblage composed dominantly of a K-Ca-rich alkali feldspar (KCRAF) intimately intergrown as semi-skeletal laths in an irreg-

ular trellis-like arrangement with needle-like grains of a silica polymorph (Fig. 1). The latter we have identified as α -quartz based on TEM electron diffraction patterns of a FIB-sectioned region of the microgranophyre.

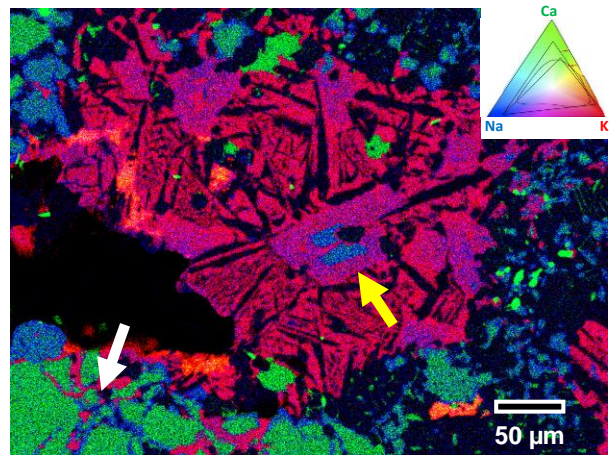


Figure 1. False-color EDS X-ray count element map showing relative distribution of **K (red)**, **Ca (green)** and **Na (blue)** in and around a felsite microgranophyre patch in 12013. Yellow arrow shows KCRAF phenocryst that has a K-free core (blue) of avg. An₅₅ plagioclase. Grains of avg. An₅₅ (blue) and An₈₅ (green) plagioclase distributed in matrix are visible, along with fracture fillings (white arrow) composed of KCRAF and avg. An₅₅ feldspars.

The KCRAF feldspar compositional distribution as determined from microprobe analyses in this study is in excellent agreement with data in [6] (Fig. 2). An additional key textural feature, first noted by [6], is that KCRAF grains occur additionally within the microgranophyre as subhedral microphenocrysts enclosed in the microgranophyre’s finer-grained alkali feldspar+quartz intergrowth. These phenocrysts in some cases also exhibit compositionally-distinct cores of a K-free plagioclase with An₅₅ average composition sharply bounded with a moderately zoned KCRAF mantle (Figs. 1&2). EDS element maps at various scales reveal that: 1) the avg. An₅₅ plagioclase composition is not restricted to the phenocryst cores, but also occurs as isolated, non-mantled grains scattered in the microgranophyre (Fig. 1), and 2) the avg. An₅₅ com-

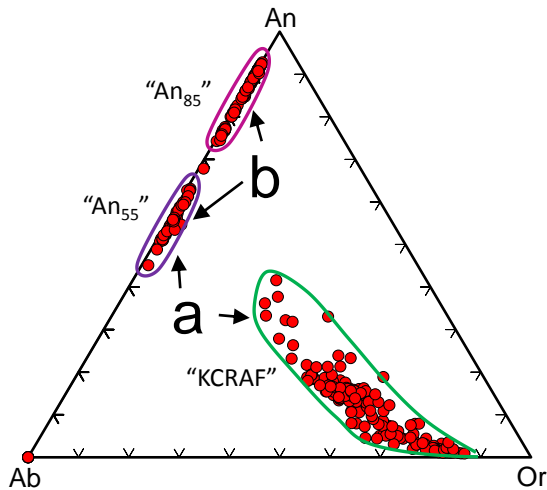


Figure 2. Microprobe analyses of feldspars hosted in: **a)** 12013 microgranophyres and fracture/void fillings (“KCRAF” and “An₅₅”) and **b)** 12013 crystalline matrix (“An₅₅” and “An₈₅”).

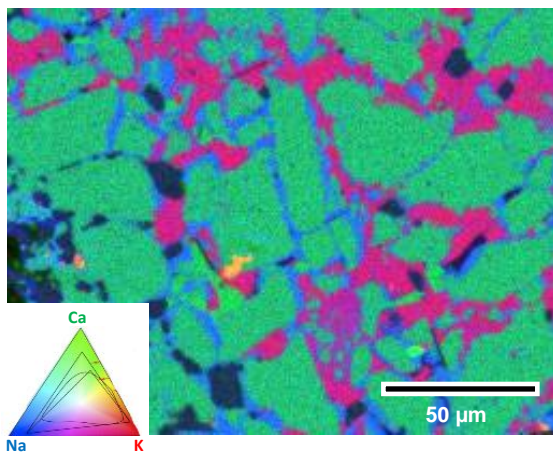


Figure 3. K-Ca-Na element map (as in Fig. 1). of KCRAF (red) and avg. An₅₅ plagioclase (blue) deposited as fracture and void fillings inside a shock-disrupted avg. An₈₅ plagioclase grain.

position makes up a significant population of grains outside the microgranophyres (Figs. 1&3). The textural relations and assemblages of the avg. An₅₅ plagioclase outside the microgranophyre specifically include: a) as isolated grains in the breccia matrix together with calcic, more typically lunar, avg. An₈₅ plagioclase (Fig. 1), b) as partial rims around the more calcic An₈₅ grains, and c) together with KCRAF and minor silica in assemblages that fill fracture networks and/or voids formed in larger grains of calcic plagioclase disrupted by shock (Figs. 1&3). The latter occurrence, also described in [7], is no less “granitic” in its overall phase assemblage than the microgranophyre itself. However, it clearly represents a unique physical context for form-

ing a granitic felsite assemblage in a lunar rock. TEM work is ongoing to identify the structural form of the silica in this unusual lunar felsite.

Discussion: The compositional trend of the KCRAF feldspars in the microgranophyre is characteristic of a one-feldspar, hypersolvus crystallization trend in a nominally dry granitic system with the liquidus at relatively high temperature (800-900°C) (Fig. 2). The avg. An₅₅ plagioclase phenocryst cores and isolated avg. An₅₅ grains within the microgranophyre show no compositional evidence of participating in this crystallization trend, and are not predicted by the relevant phase relations. They most likely represent xenocrysts introduced at various stages before or during microgranophyre crystallization, possibly from the population of An₅₅ grains in the surrounding rock. The fact that these xenocrysts are linked, at least compositionally, to the larger population of compositionally distinct avg. An₅₅ plagioclases found in different microstructural contexts throughout the breccia is intriguing. It suggests, in particular, that granophyre formation followed sequentially after, or closely associated with, one or more of the events that formed grains in the avg. An₅₅ compositional population. Notably, one of these events involved the crystallization of avg. An₅₅ plagioclase associated with KCRAF feldspars as fracture infillings within coarser grained avg. An₈₅ plagioclase grains previously disrupted by shock. This would have necessitated conditions allowing a parent liquid or carrier fluid phase to infiltrate the intricate micron-scale fracture spacings. The same infiltrating fluid may also account for the crystallization or replacement reaction that form the rims of An₅₅ plagioclase rims around the more calcic avg. An₈₅ in the breccia matrix.

In summary, we have found evidence that alkali components were mobilized at one or more stages in the formation of the 12013 breccia, allowing evolved felsite assemblages to crystallize under conditions that may not have been conventionally igneous. A role for a carrier phase, either a high-temperature low-viscosity silicate liquid, or supercritical fluid is indicated. The implications of such a carrier phase for controlling the inventory of water and volatiles in this and other similar felsite-containing lunar breccias will require careful assessment in future studies of lunar volatiles.

References: [1] Mills R. D. et al. (2017) *Geochem. Persp. Lett.*, 3, 115-123. [2] Simon J. I. et al. (2017) *LPS XLVIII*, Abstract #1248. [3] Hui et al. (2013) *Nature Geoscience*, 6, 177-180. [4] Mosenfelder et al. (2017) (2017) *LPS XLVIII*, Abstract #2473. [5] Seddio S. M. et al. (2015) *Am. Min.*, 100, 1533-1543. [6] Quick J. E. et al. (1981) *Proc. Lunar Planet. Sci.*, 12B, 117-172. [7] Mouser, M. et al. (2018) *this meeting*.